

# Hydrogen Bond Contribution to Preferential Solvation in $S_NAr$ Reactions

Rodrigo Ormazabal-Toledo,<sup>\*,†</sup> José G. Santos,<sup>‡</sup> Paulina Ríos,<sup>‡</sup> Enrique A. Castro,<sup>‡</sup> Paola R. Campodónico,<sup>§</sup> and Renato Contreras<sup>\*,†</sup>

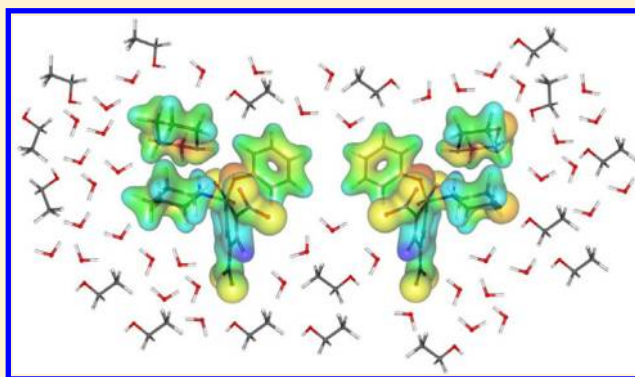
<sup>†</sup>Departamento de Química, Facultad de Ciencias, Universidad de Chile, Casilla 653, Santiago, Chile

<sup>‡</sup>Facultad de Química, Pontificia Universidad Católica de Chile, Casilla 306, Santiago 6094411, Chile

<sup>§</sup>Instituto de Ciencias, Facultad de Medicina, Clínica Alemana Universidad del Desarrollo, Santiago 7710162, Chile

## S Supporting Information

**ABSTRACT:** Preferential solvation in aromatic nucleophilic substitution reactions is discussed using a kinetic study complemented with quantum chemical calculations. The model system is the reaction of a series of secondary alicyclic amines toward phenyl 2,4,6-trinitrophenyl ether in aqueous ethanol mixtures of different compositions. From solvent effect studies, it is found that only piperidine is sensitive to solvation effects, a result that may be traced to the polarity of the solvent composition in the ethanol/water mixture, which points to a specific electrophilic solvation in the aqueous phase.



## INTRODUCTION

According to Ben-Naim<sup>1</sup> and other authors,<sup>2–5</sup> preferential solvation may be defined as the difference between the local and bulk composition of the solute with respect to the various components of the solvent, in this case, a binary water/ethanol mixture. The bulk solvation effects may in general be assessed using continuum dielectric models framed on the classical Kirkwood–Onsager theories<sup>1,6,7</sup> or using a quantum mechanical model of solvation based on the reaction field theory.<sup>8,9</sup> If we assume that the bulk solvation properties of a mixture of polar protic solvents may be described by an average of the effective dielectric constants, preferential solvation may be cast into the form of specific solute–solvent interactions describing local solvation, which we may define as a “first solvation shell”. Local solvation may be further classified as “electrophilic” or “nucleophilic”.<sup>10–13</sup> For a solvent mixture of the general form ROH (R = H or Et), electrophilic solvation represents the specific interaction through a H-bond with the hydrogen atom of the solvent, whereas nucleophilic solvation describes a specific interaction through a H-bond between an acidic hydrogen atom of the solute and the heteroatom (oxygen in this case) of the solvent.

Preferential solvation may result in dramatic changes in reaction mechanisms. Several examples of this have been reported for the solvolysis of fluorinated alcohols in trifluoroethanol/water and trifluoroethanol/ethanol mixtures,<sup>11</sup>  $S_N2$  reactions of sodium 4-nitrophenoxide and iodomethane in an acetone/water mixture,<sup>14</sup> and solvolysis of acetyl chloride in methanol/acetone, methanol/acetonitrile, and methanol/etha-

nol mixtures.<sup>15</sup> Preferential solvation of 1-halo-2,4-dinitrobenzenes in aromatic nucleophilic substitution reactions with several amines has also been reported by Mancini et al. in mixtures of dichloromethane with different polar protic and polar aprotic cosolvents.<sup>16–22</sup>

In this work, we report an integrated experimental and theoretical study of the title reactions, to discuss preferential solvation effects from an electronic point of view. The theoretical model is developed in terms of electron density-dependent descriptors of reactivity. The model system is the reaction of phenyl 2,4,6-trinitrophenyl ether (1) with a series of secondary alicyclic (SA) amines (2–6), depicted in Scheme 1.

The  $S_NAr$  reaction occurs in activated substrates, generally possessing aromatic rings strongly activated by electron-withdrawing substituents.<sup>23–25</sup> In some of the studied reactions involving highly activated substrates, two types of kinetic data have been recorded:<sup>26</sup> one showing the rapid increase in the magnitude of a band near 500 nm associated with a  $\sigma$ -complex formed by the addition of the nucleophile to one of the unsubstituted positions of the aromatic ring and the other showing the decrease in the magnitude of a band corresponding to the disappearance of the substrate and an increase in the magnitude of another band corresponding to the final product.<sup>26</sup> It is noteworthy that in most  $S_NAr$  processes the

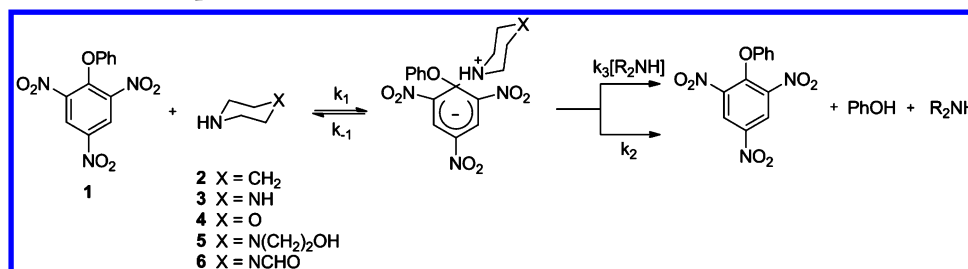
Received: January 16, 2013

Revised: April 17, 2013

Published: April 18, 2013



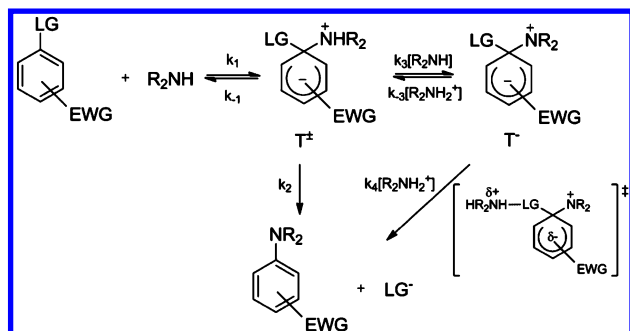
**Scheme 1.** General Mechanism for a  $S_NAr$  Reaction of Secondary Alicyclic Amines as Nucleophiles toward Phenyl 2,4,6-Trinitrophenyl Ether as an Electrophile



former reaction is not observed. The overall pathway for these reactions with amines as nucleophiles is shown in Scheme 1.<sup>27</sup>

According to Scheme 1, the first step is the formation of a  $\sigma$ -complex that occurs after amine attack to the substituted aromatic ring. In a second step, the  $\sigma$ -complex leads to products by a catalyzed ( $k_3$ ) or noncatalyzed ( $k_2$ ) route. The process involves the loss of aromaticity in step 1 and rearomatization in step 2. For this type of reaction, it is possible that an equilibrium may be reached between the zwitterionic  $\sigma$ -complex ( $T^\pm$ ) and its deprotonated form, the anionic  $\sigma$ -complex ( $T^-$ ),<sup>28</sup> followed by its general acid catalysis conversion to products, as shown in Scheme 2.

**Scheme 2.** Possible Pathways for a  $S_NAr$  Reaction Involving a Secondary Amine

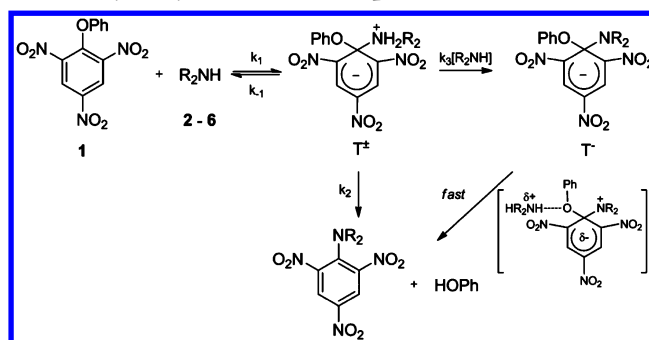


When the  $k_4$  step is rate-determining, this reaction pathway is called the specific base–general acid mechanism (SB–GA mechanism).<sup>29,30</sup> On the other hand, when the transfer of the proton from the zwitterionic intermediate is rate-limiting, followed by the rapid loss of the leaving group, the mechanism is named rate-limiting proton transfer (RLPT).<sup>23,28,31</sup>

## RESULTS AND DISCUSSION

Under the experimental conditions used, the formation of a single product was spectrophotometrically observed. Therefore, the possibility of nucleophilic attack at the unsubstituted ring positions may be safely discarded. For the reactions of **1** with the SA amine series in aqueous ethanol mixtures, the plots of  $k_{\text{obs}}$  against free amine concentration ( $[N]_F$ ) are in accordance with a second-order polynomial equation (see Figures S1–S4 of the Supporting Information). The results are in agreement with Scheme 3, which is similar to Scheme 2, but assuming  $k_4 \gg k_{-3}$ . In Scheme 3, the loss of a proton from the zwitterionic intermediate is the rate-limiting step (i.e., RLPT mechanism) and not the expulsion of the phenoxide from the anionic intermediate.

**Scheme 3.** RLPT Mechanism for the Reaction of **1** with Secondary Alicyclic Amines in Aqueous Ethanol Mixtures



Via application of the steady state condition to the intermediates, eq 1 can be derived, where  $[N]_F$  is the free amine concentration.

$$k_{\text{obs}} = \frac{k_1 k_2 [N]_F + k_1 k_3 [N]_F^2}{k_{-1} + k_2 + k_3 [N]_F} \quad (1)$$

Assuming that  $k_2 + k_3 [N]_F \ll k_{-1}$ , eq 1 can be simplified to eq 2, where  $K_1 = k_1/k_{-1}$ .

$$k_{\text{obs}} = K_1 k_2 [N]_F + K_1 k_3 [N]_F^2 \quad (2)$$

Plots of  $k_{\text{obs}}$  versus  $[N]_F$  were curved upward for all the amines studied, in accordance with eq 2. These kinetic data were fit to eq 2, and the resulting curves are shown in Figures S1–S4 of the Supporting Information. The good fits reinforce the fact that the second step in Scheme 3 is dual: catalyzed and noncatalyzed pathways. For the reactions with all SA amines, except piperidine, the plots described above were found to be independent of the composition of the solvent mixture, within the range studied [25, 50 and 75% (v/v) ethanol]. Namely, a single parabolic curve is shown for the reactions in the different mixtures. In contrast, the plots of  $k_{\text{obs}}$  versus  $[N]_F$  for the reaction with piperidine are shown in Figure 1. It can be observed that in the presence of increasing water content, the rate coefficients increase, thereby suggesting an increasing degree of stabilization of the  $T^\pm$  complex by a preferential solvation in the aqueous phase.

By non-least-squares fitting of eq 2 to the experimental points, the values of  $K_1 k_2$  and  $K_1 k_3$  were found for all the SA amines. These are listed in Table 1. Figure 2 shows the Brønsted-type plots for the  $K_1 k_2$  and  $K_1 k_3$  values obtained for the reactions of the SA amine series with ether **1**. These plots are linear with slopes  $\beta_{Kk_3} = 1.05$  for  $K_1 k_3$  and  $\beta_{Kk_2} = 0.80$  for  $K_1 k_2$ , which is in agreement with the stepwise mechanism shown in Scheme 3, where the proton transfer is the rate-determining step.

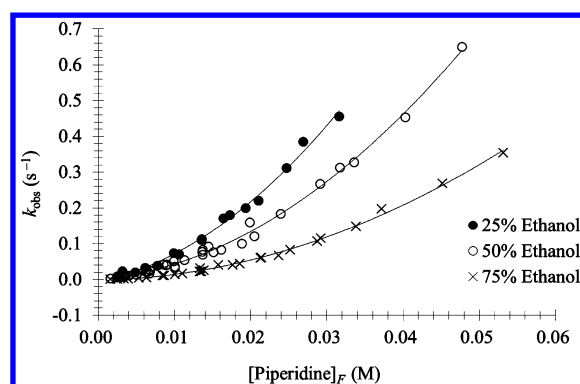


**Figure 1.** Plot of  $k_{\text{obs}}$  vs free piperidine concentration ( $[\text{piperidine}]_F$ ) for the piperidinolysis of **1**, in 25, 50, and 75% (v/v) ethanol aqueous mixtures, at 25 °C and an ionic strength of 0.2 M (KCl).

To prove the hypothesis of a preferential solvation by water in the reaction with piperidine, we first evaluated the electrophilic and nucleophilic sites in ethanol and water. The local electrophilicity<sup>32</sup> and nucleophilicity<sup>33</sup> of the solvents are approached as

$$\omega_G^+ = \sum_{k \in G} f_k^+ \omega^+; \quad \omega^+ = \frac{\mu^2}{2\eta} \quad (3)$$

$$\omega_G^- = \sum_{k \in G} f_k^- \omega^-; \quad \omega^- = \varepsilon_{\text{HOMO}} \quad (4)$$

These are expressed in terms of the electronic chemical potential ( $\mu$ ) and the chemical hardness ( $\eta$ ).<sup>34</sup> The regional (or group) quantities are projected by using the appropriate electrophilic and nucleophilic Fukui functions  $f_k^+$  and  $f_k^-$ , respectively, using a method described elsewhere.<sup>35,36</sup> The electronic chemical potential and the chemical hardness were obtained using the frontier molecular orbital HOMO and LUMO.<sup>34</sup>

Using eqs 3 and 4, we found that the local electrophilicities at the hydrogen acidic atom of water and ethanol are 0.35 and 0.21 eV, respectively. Local nucleophilicity at the heteroatom site of the solvent on the other hand yields values of 13.30 and 6.51 eV for water and ethanol, respectively. These results show that both electrophilic solvation and nucleophilic solvation play a significant role in favor of preferential aqueous phase solvation. To qualitatively explore the sites that are more likely to be electrophilically and nucleophilically bound by water molecules, we performed a molecular electrostatic potential (MEP) calculation for the transition state structures involved in the reactions being studied (see the computational details section in the Supporting Information).

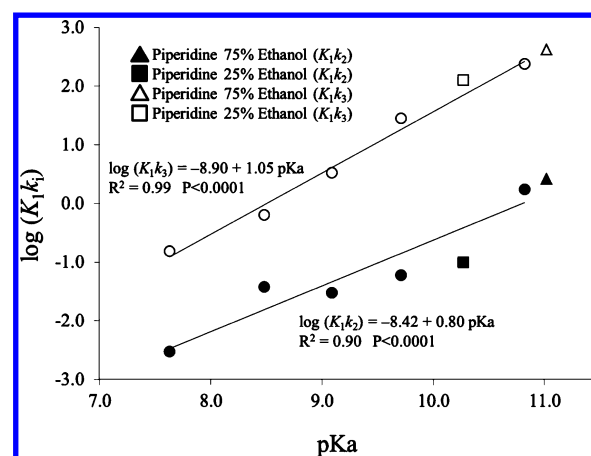


**Figure 2.** Brønsted-type plots for the reaction of **1** with SA amines. Filled circles depict data for the catalyzed pathway and empty circles data for the uncatalyzed pathway.

Figure 3 illustrates the molecular electrostatic potential (MEP) plot for the transition state (TS) structure corresponding to the nucleophilic attack of morpholine and piperidine on ether **1**. Figure 3 shows that both structures differ only in the substituent at position 4 (with respect to the nucleophilic center). The arrow highlights the position of the substituent at the amine moiety. The orientation of the amine relative to the substrate is almost conserved along the whole reaction path (IRC profile). This substitution pattern is responsible for the different distribution of the electron density.

Figure 3 also shows that for morpholine, a negative zone in the MEP (green colored) appears over the oxygen atom. However, for piperidine, the negative zone is dramatically diminished. The remaining structure is almost the same for both amines. This result is relevant because this behavior is probably responsible for the different interactions between the transition state and the solvent mixture. It is noteworthy that the kinetic experiments give information about only the rate-determining step ( $k_3$  step in Scheme 3). Figure 3 adds information related to the first step of the reaction, which is structurally maintained along the whole reaction profile, as discussed later.

It is worth emphasizing that the series of amines **3–6** display patterns of MEP similar to that of morpholine (see Figures S5–S7 of the Supporting Information for the remaining amines). Note that while for morpholine and amines **3–6** there is a net site at position 4 of the nucleophile ring amenable to electrophilic solvation, in structure b of Figure 3 corresponding to piperidine, the system may accept an electrophilic or nucleophilic H-bond, or both, from the solvent. If we consider

**Table 1.** Values of  $K_1k_2$  and  $K_1k_3$  for the Reaction of SA Amines with **1** in Different Aqueous Ethanol Mixtures at 25 °C and an Ionic Strength of 0.2 M (KCl)

nucleophile	pK <sub>a</sub> <sup>a</sup>	pK <sub>a</sub> <sup>b</sup>	pK <sub>a</sub> <sup>c</sup>	$K_1k_2$ (M <sup>-1</sup> s <sup>-1</sup> )	$K_1k_3$ (M <sup>-1</sup> s <sup>-2</sup> )
2	11.02	—	—	2.59 ± 0.45	416.71 ± 25.84
2	—	10.82	—	1.75 ± 0.19	240.53 ± 10.93
2	—	—	10.27	0.10 ± 0.06	128.01 ± 2.73
3	9.86	9.71	9.61	0.06 ± 0.01	28.33 ± 0.63
4	9.16	9.09	8.88	0.03 ± 0.002	3.36 ± 0.09
5	8.56	8.48	8.23	0.038 ± 0.004	0.637 ± 0.06
6	7.71	7.63	7.47	0.003 ± 0.001	0.154 ± 0.02

<sup>a</sup>In a 25% (v/v) ethanol aqueous mixture. <sup>b</sup>In a 50% (v/v) ethanol aqueous mixture. <sup>c</sup>In a 75% (v/v) ethanol aqueous mixture.

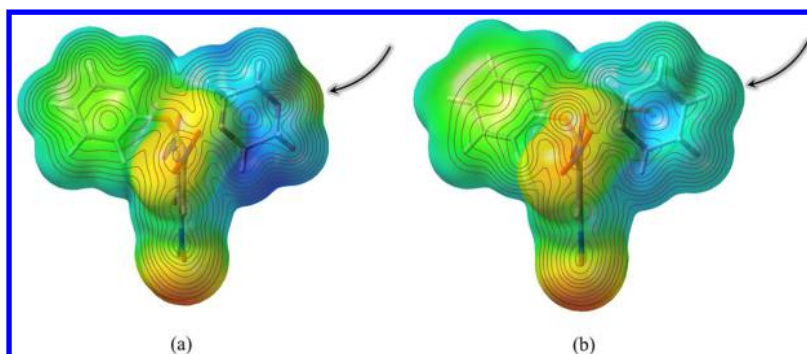


**Figure 3.** MEP surface corresponding to the TS structure for the formation of the  $T^\pm$  intermediate for the reaction of **1** toward morpholine (a) and piperidine (b). Arrows point to position 4 of the nucleophile. Nucleophilic sites are colored red and electrophilic ones blue. Green zones are regions of vanishing MEP values.

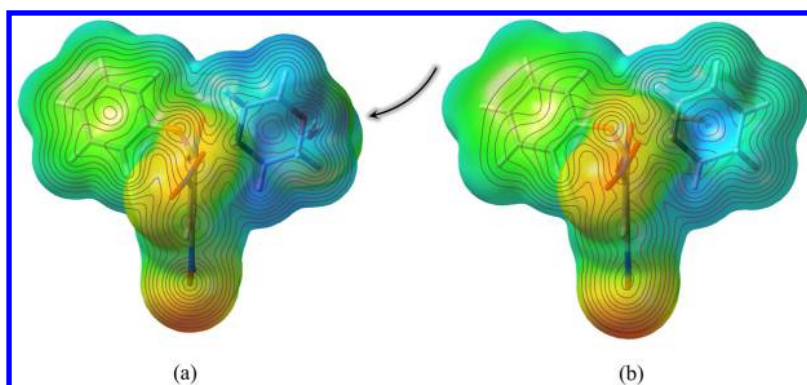


**Figure 4.** MEP surface corresponding to the TS structure for the formation of the  $T^\pm$  intermediate for the reaction of **1** toward morpholine (a) and piperidine (b). Arrow points to position 4 in the nucleophile. In piperidine, the water molecule is stabilized by the *o*-NO<sub>2</sub> behind the plane. Nucleophilic sites are colored red and electrophilic ones blue. Green zones are regions of vanishing MEP values.

that ethanol and water show comparable values of local electrophilicity at the hydrogen atom, site 4 may be equally disposed to accept binding to either water or ethanol, and in this sense, there is no selectivity toward electrophilic solvent binding. However, in piperidine, there is no preferential affinity for an electrophilic or nucleophilic attachment of solvent molecules. This means that in piperidine the solvent may bond the transition state via a hydrogen bond in the electrophilic or nucleophilic solvation mode. Because the regional nucleophilicity of water is approximately twice that of ethanol, it may be concluded that preferential solvation at the TS stage of the reaction is driven by the nucleophilic solvation by water.

The effect of solvent on the kinetics for the reactions with piperidine, summarized in Figure 1, may be attributed to a different molecular interaction between piperidine and solvent molecules.<sup>37</sup> These results show that the environment of the Meisenheimer complex (MC) changes for different solvent compositions. Nevertheless, for the remaining amines, the environment of the MC is similar because of the polar nature of the substituents at position 4, thereby suggesting that their kinetic responses are rather independent of the bulk properties of the solvent.

Figure 4 shows the MEP at the transition state for morpholine and piperidine and their possible H-bond complexes formed with the corresponding amine and a water molecule. These are the interactions expected for the rate-determining step in Scheme 3. Note that for morpholine, the presence of a water molecule bound to position 4 of the nucleophile moiety at the transition state results in a

nucleophilic deactivation at that site. This effect not only arises from steric hindrance but also may be induced by electron density reorganization in the whole structure (electrophilic solvation effect). This effect may be seen by comparing Figure 3a with the corresponding structure shown in Figure 4a. It is also interesting to note that for piperidine, in the presence of a water molecule bound to the O atom in the ortho-nitro moiety, the electrophilic solvation induces a marginal electronic effect on the whole structure at the transition state. We must emphasize that the position of the water molecule in this case also represents a true stationary point on the potential energy surface. Note that comparison of panels a and b of Figure 4 also stresses a nucleophilic activation in the former.

The results obtained by a full exploration of the potential energy surface are consistently in agreement with the kinetic study. From Table 1, it may be seen that for piperidine, the rate coefficient increases when the polarity of the reaction media is increased. This result highlights the relevance of a protic reaction medium on the reaction mechanism, specifically, on the step involving proton transfer processes. In this reaction pathway, the water molecules compete with the nucleophile (the catalyzed pathway) for proton abstraction. It seems that a less favorable proton transfer toward water molecules, compared to proton transfer toward the second catalyzing nucleophile, drives the reaction mechanism for the whole series of amines considered in this study.

Note that for amines **3–6**, the kinetic study suggests that solvation effects of reaction media of varying polarity have a



marginal effect on the reaction rates (see the Supporting Information for a detailed description of the kinetic study).

Additionally, the change in the rate constants may be induced by a hyperconjugative effect around the TS stage. The interaction between the substituent in position 4 in the nucleophile and the hydrogen atom that is transferred to the phenoxide group in the rate-limiting step is favored. Consequently, when piperidine is the nucleophile, the interaction is less favorable, destabilizing the  $T^\ddagger$  intermediate and powering the proton transfer. With the other amines, the situation is similar: when the hyperconjugative effect is dominant, the  $T^\ddagger$  intermediate is more stable and the proton loss is a slower process as for the 1-formylpiperazine nucleophile.

Table 2 displays the main specific interactions evaluated at the TS stage of the reaction under study. These interactions

**Table 2. Second-Order Perturbation Theory Analysis for the Reaction between 1 and the Full Set of SAA<sup>a</sup>**

nucleophile	donor	acceptor	$E^{(2)}$
2	LP(O <sub>1</sub> )	BD*(N <sub>2</sub> –H <sub>3</sub> )	8.5
3	LP(O <sub>1</sub> )	BD*(N <sub>2</sub> –H <sub>3</sub> )	9.4
4	LP(O <sub>1</sub> )	BD*(N <sub>2</sub> –H <sub>3</sub> )	8.9
5	LP(O <sub>1</sub> )	BD*(N <sub>2</sub> –H <sub>3</sub> )	11.0
6	LP(O <sub>1</sub> )	BD*(N <sub>2</sub> –H <sub>3</sub> )	12.6

<sup>a</sup>The interactions presented are those depicted in Scheme 4a. Energies are in kilocalories per mole.

have been calculated by performing a second-order perturbation theory calculation using the NBO analysis.<sup>38–40</sup> Second-order perturbation theory analysis is a tool that provides detailed microscopic information from a localized antibonding orbital (NBO) analysis of an idealized Lewis structure with an empty non-Lewis orbital (see Tables 2 and 3). For each donor and acceptor orbitals  $i$  and  $j$  say, the energy of stabilization is denoted by  $E^{(2)}$  and is evaluated as

$$E^{(2)} = \Delta E_{ij} = q_i \frac{F(i, j)^2}{\epsilon_j - \epsilon_i} \quad (5)$$

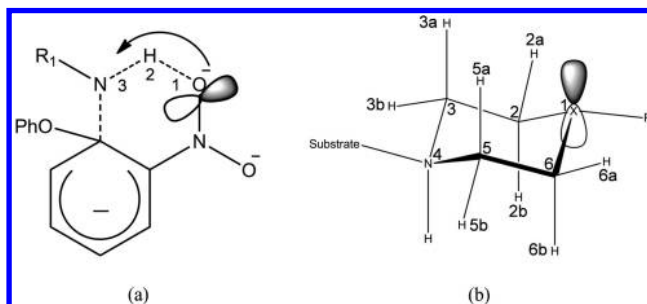
**Table 3. Second-Order Perturbation Theory Analysis for the Reaction between 1 and the Full Set of SAA<sup>a</sup>**

interaction		nucleophile <sup>b</sup>				
donor	acceptor	3	4	5 <sup>c</sup>	5 <sup>d</sup>	6
LP(X <sub>1</sub> )	BD*(C <sub>2</sub> –C <sub>3</sub> )	7.5	7.8	0.9	5.4	4.1
LP(X <sub>1</sub> )	BD*(C <sub>5</sub> –C <sub>6</sub> )	8.0	8.2	1.1	5.7	4.0
LP(X <sub>1</sub> )	BD*(C <sub>2</sub> –H <sub>2a</sub> )	2.6	3.0	0.8	6.1	6.5
LP(X <sub>1</sub> )	BD*(C <sub>2</sub> –H <sub>2b</sub> )	0.8	0.8	2.6	<0.5	<0.5
LP(X <sub>1</sub> )	BD*(C <sub>3</sub> –H <sub>3a</sub> )	0.6	<0.5	<0.5	0.6	0.5
LP(X <sub>1</sub> )	BD*(C <sub>3</sub> –H <sub>3b</sub> )	<0.5	<0.5	<0.5	<0.5	<0.5
LP(X <sub>1</sub> )	BD*(C <sub>5</sub> –H <sub>5a</sub> )	2.8	3.3	0.8	6.4	6.3
LP(X <sub>1</sub> )	BD*(C <sub>5</sub> –H <sub>5b</sub> )	0.7	0.6	2.6	<0.5	<0.5
LP(X <sub>1</sub> )	BD*(C <sub>6</sub> –H <sub>6a</sub> )	0.6	<0.5	<0.5	0.6	0.5
LP(X <sub>1</sub> )	BD*(C <sub>6</sub> –H <sub>6b</sub> )	<0.5	<0.5	<0.5	<0.5	<0.5

<sup>a</sup>The interactions and labeling presented are that depicted in Scheme 4b. Energies are in kilocalories per mole. <sup>b</sup>Piperidine is not included in this table because the interactions described are all near zero. <sup>c</sup>Interaction formed between the axial nonbonding orbital with the antibonding orbital series. <sup>d</sup>Interaction formed between the equatorial nonbonding orbital with the antibonding orbital series.

where  $q_i$  is the donor orbital occupancy,  $\epsilon_i$  and  $\epsilon_j$  are diagonal elements, and  $F(i, j)$  is the off-diagonal elements of the Fock matrix. The main interactions presented are those depicted in Scheme 4.

**Scheme 4. Possible Interactions between the Electrophile and Nucleophile Centers<sup>a</sup>**



<sup>a</sup>Irrelevant atoms were omitted. (a) Hydrogen bond between the oxygen's lone pairs in the  $o$ -NO<sub>2</sub> group and the N–H antibonding orbital of the nucleophilic center and (b) interaction between the substituent at position 4 in the nucleophile and antibonding orbitals of the amine (see the text for details).

From the information listed in Table 2, it is possible to note that the main interaction is that established between the acidic hydrogen atom in the nucleophilic center and the  $o$ -NO<sub>2</sub> group in the substrate.<sup>41–43</sup> On the other hand, the homoanomeric effect<sup>44–48</sup> that may be present in the nucleophile is weaker than the interaction between the nucleophile and the electrophile. Nevertheless, the energy values observed are within the range previously reported.<sup>48</sup> In this sense, the nucleophile–electrophile interactions together with the preferential solvation effects are the dominant stabilizing effects induced in this type of reaction, and these effects outweigh the homoanomeric effect present in the nucleophilic ring.

Table 3 displays the interactions between the lone pair in the heteroatom and different possible accepting orbitals in the nucleophile. These interactions have been reported to be relevant for the description of reactivity trends.<sup>49</sup> For instance, when we take into account the interaction between the lone pair in the nitrogen atom [LP(X<sub>1</sub>)] and the antibonding orbital C<sub>2</sub>–C<sub>3</sub>, it is possible to note the following features: this interaction diminishes the energy value downward with the pK<sub>a</sub>, thereby suggesting that it is relevant for assisting the nucleophilic attack. Similar results are obtained for the interaction between the lone pair in the nitrogen atom [LP(X<sub>1</sub>)] and the antibonding orbital associated with the C<sub>5</sub>–C<sub>6</sub> bond. On the other hand, for the interaction between the LP(X<sub>1</sub>) orbital and the C<sub>i</sub>–H<sub>j</sub> antibonding orbitals, an opposite trend is obtained: a more efficient interaction of this kind diminishes the reactivity of the system. Consider, for instance, the interactions involving the BD\*(C<sub>2</sub>–H<sub>2a</sub>). In this case, the  $E^{(2)}$  value increases and the nucleophilicity of the amine decreases. In the case of morpholine, the situation is the same, but this time, the interaction is established between the two lone pairs in the oxygen atom. Note that one orbital is axially oriented while the other is equatorial (see Table 3). The interactions are different for both orbitals, but in the global analysis, they can be taken as additive contributions.<sup>49</sup>

Finally, piperidine does not establish any of the interactions discussed above. This result may be traced to the presence of a methylene group at position 4 that does not bear any lone pair

that could interact with other sites of the amine. Note that in this case, the electrophilic solvation will become more important, in agreement with the experimental observations. In summary, the orbital interaction analysis quoted in Table 3 nicely complements the experimental results and can be used to further provide a semiquantitative hierarchy of nucleophilicity for the series of amines studied in this work.

## CONCLUSIONS

The reactions of a series of secondary alicyclic amines toward phenyl 2,4,6-trinitrophenyl ether in aqueous ethanol mixtures of different compositions have been examined at the experimental and theoretical levels to understand specific solvation effects on the reaction mechanism of the title reactions. It is found that only piperidine is sensitive to solvation effects, a result that may be traced to the polarity of the solvent composition in the ethanol/water mixture that points to a specific electrophilic solvation in the aqueous phase. The electronic analysis based on the MEP highlights the effects that the substituent at the nucleophiles may exert on the solute–solvent interactions in these systems.

## EXPERIMENTAL SECTION

**Materials.** Amines were purified by distillation or recrystallization, except piperazine, which was purified by sublimation. The substrate, phenyl 2,4,6-trinitrophenyl ether (**1**), was prepared by the method described previously<sup>16–19</sup> [mp 157.1–158.7 °C (lit. 155–156 °C)]. The solid, recrystallized from chloroform, was identified by the following NMR properties: <sup>1</sup>H NMR (400 MHz, CDCl<sub>3</sub>)  $\delta$  6.91 (d, 2H,  $J$  = 7.9 Hz), 7.21 (m, 1H,  $J$  = 7.3 Hz), 7.34 (d, 2H,  $J$  = 8.1 Hz), 8.97 (s, 2H); <sup>13</sup>C NMR (400 MHz, CDCl<sub>3</sub>)  $\delta$  115.9 (CH), 124.5 (CH), 125.3 (CH), 130.3 (CH), 142.5 (C-2/6), 144.5 (C-4), 146.9 (C-1), 156.1 (C-7).

**Kinetic Measurements.** These data were recorded spectrophotometrically (330–550 nm range) by means of a diode array spectrophotometer in ethanol aqueous mixtures, at 25.0  $\pm$  0.1 °C, an ionic strength of 0.2 M (KCl), and three different pH values maintained by partial protonation of the amines. The reactions, studied under an excess of the amine over the substrate, were started by injection of a substrate stock solution in acetonitrile (10  $\mu$ L) into the amine aqueous ethanol solution (2.5 mL in the spectrophotometric cell). The initial substrate concentration was  $\sim 1 \times 10^{-4}$  M. Pseudo-first-order rate coefficients ( $k_{\text{obs}}$ ) were found for all reactions; these were determined by means of the spectrophotometer kinetic software for first-order reactions at 385–390 nm, corresponding to 2,4,6-trinitro-1-aminobenzene. The experimental conditions of the reactions and the  $k_{\text{obs}}$  values are listed in Tables S1–S15 of the Supporting Information.

**Product Analysis.** For the studied reactions, the increase in the magnitude of a band centered at 385–390 nm was observed; this band is attributed to the corresponding 2,4,6-trinitro-1-aminobenzene. The final product of the reaction with morpholine was identified as 2,4,6-trinitro-*N*-morpholinobenzene. This was achieved by comparison of the UV–vis spectrum after completion of this reaction with that of an authentic sample<sup>20</sup> under the same conditions ( $\beta_{\text{max}}$  = 388 nm).

**Computational Details.** Cartesian coordinates, energies, and the number of imaginary frequencies for stationary points are compiled in the Supporting Information. The transition state structures were obtained at the B3LYP/6-311+G(d,p)

level of theory. In addition to the optimized structure, a water molecule was coordinated and the system was relaxed at the same level of theory as the previous system. To identify stationary points as transition state structures, we performed harmonic analysis to check the presence of a unique imaginary frequency at the same level of theory. All the calculations were performed using the Gaussian 03 suite of programs.<sup>50</sup>

## ASSOCIATED CONTENT

### Supporting Information

Kinetic results (Tables S1–S15), plots of  $k_{\text{obs}}$  versus  $[N]_{\text{F}}$  for all the reactions (Figures S1–S4), <sup>1</sup>H and <sup>13</sup>C NMR spectra for phenyl 2,4,6-trinitrophenyl ether and the final product 2,4,6-trinitro-1-morpholinobenzene, Cartesian coordinates, energies, and the number of imaginary frequencies (NIMAG) considered in this study (Tables S16–S26), and the complete ref S0. This material is available free of charge via the Internet at <http://pubs.acs.org>.

## AUTHOR INFORMATION

### Corresponding Author

\*E-mail: [rcontrer@uchile.cl](mailto:rcontrer@uchile.cl). Phone: (+56 2) 29787272. Fax: (+56 2) 2713888.

### Notes

The authors declare no competing financial interest.

## ACKNOWLEDGMENTS

This work was supported by Project ICM- P10-003-F CILIS, granted by Fondo de Innovación para la Competitividad del Ministerio de Economía, Fomento y Turismo, Chile, and Fondecyt Grants 1100492, 1110062, and 1095145. R.O.-T. thanks CONICYT of Chile for a doctoral fellowship.

## REFERENCES

- (1) Ben-Naim, A. Preferential Solvation in Two- and in Three-component Systems. *Pure Appl. Chem.* **1990**, *62*, 25–34.
- (2) Covington, A. K.; Newman, K. E. Approaches to the Problems of Solvation in Pure Solvents and Preferential Solvation in Mixed Solvents. *Pure Appl. Chem.* **1979**, *51*, 2041–2058.
- (3) Langford, C. H.; Tong, J. P. K. Preferential Solvation and the Role of Solvent in Kinetics. Examples from Ligand Substitution Reactions. *Acc. Chem. Res.* **1977**, *10*, 258–264.
- (4) Petrov, N. K.; Wiessner, A.; Staerk, H. A Simple Kinetic Model of Preferential Solvation in Binary Mixtures. *Chem. Phys. Lett.* **2001**, *349*, 517–520.
- (5) Salari, H.; Khodadadi-Moghaddam, M.; Harifi-Mood, A. R.; Gholami, M. R. Preferential Solvation and Behavior of Solvatochromic Indicators in Mixtures of an Ionic Liquid with Some Molecular Solvents. *J. Phys. Chem. B* **2010**, *114*, 9586–9593.
- (6) Kirkwood, J. G. Theory of Solutions of Molecules Containing Widely Separated Charges with Special Application to Zwitterions. *J. Chem. Phys.* **1934**, *2*, 351–361.
- (7) Onsager, L. Electric Moments of Molecules in Liquids. *J. Am. Chem. Soc.* **1936**, *58*, 1486–1493.
- (8) Tapia, O.; Goscinski, O. Self-consistent Reaction Field Theory of Solvent Effects. *Mol. Phys.* **1975**, *29*, 1653–1661.
- (9) Tomasi, J.; Mennucci, B.; Cammi, R. Quantum Mechanical Continuum Solvation Models. *Chem. Rev.* **2005**, *105*, 2999–3093.
- (10) Olah, G. A.; Klumpp, D. A. Superelectrophilic Solvation. *Acc. Chem. Res.* **2004**, *37*, 211–220.
- (11) Bentley, T. W.; Llewellyn, G.; Ryu, Z. H. Solvolytic Reactions in Fluorinated Alcohols. Role of Nucleophilic and Other Solvation Effects. *J. Org. Chem.* **1998**, *63*, 4654–4659.
- (12) Schadt, F. L.; William Bentley, T.; Schleyer, P. V. R. The SN2–SN1 Spectrum. 2. Quantitative Treatments of Nucleophilic Solvent

Assistance. A Scale of Solvent Nucleophilicities. *J. Am. Chem. Soc.* **1976**, *98*, 7667–7674.

(13) Winstein, S.; Grunwald, E.; Walter Jones, H. The Correlation of Solvolysis Rates and the Classification of Solvolysis Reactions into Mechanistic Categories. *J. Am. Chem. Soc.* **1951**, *73*, 2700–2707.

(14) Humeres, E.; Nunes, R. J.; Machado, V. G.; Gasques, M. D. G.; Machado, C. Ion-dipole SN2 Reaction in Acetone–Water Mixtures. Electrostatic and Specific Solute–Solvent Interactions. *J. Org. Chem.* **2001**, *66*, 1163–1170.

(15) Bentley, T. W.; Llewellyn, G.; McAlister, J. A. SN2 Mechanism for Alcoholysis, Aminolysis, and Hydrolysis of Acetyl Chloride. *J. Org. Chem.* **1996**, *61*, 7927–7932.

(16) Mancini, P. M.; Terenzani, A.; Adam, C.; Pérez, A. D. C.; Vottero, L. R. Characterization of Solvent Mixtures: Preferential Solvation of Chemical Probes in Binary Solvent Mixtures of Polar Hydrogen-bond Acceptor Solvents with Polychlorinated Co-solvents. *J. Phys. Org. Chem.* **1999**, *12*, 713–724.

(17) Mancini, P. M. E.; Terenzani, A.; Adam, C.; Pérez, A.; Vottero, L. R. Characterization of Solvent Mixtures. Part 8. Preferential Solvation of Chemical Probes in Binary Solvent Systems of a Polar Aprotic Hydrogen-bond Acceptor Solvent with Acetonitrile or Nitromethane. Solvent Effects on Aromatic Nucleophilic Substitution Reactions. *J. Phys. Org. Chem.* **1999**, *12*, 207–220.

(18) Mancini, P. M. E.; Terenzani, A.; Adam, C.; Vottero, L. R. Solvent Effects on Aromatic Nucleophilic Substitution Reactions. Part 9. Special Kinetic Synergistic Behavior in Binary Solvent Mixtures. *J. Phys. Org. Chem.* **1999**, *12*, 430–440.

(19) Mancini, P. M. E.; Terenzani, A.; Adam, C.; Vottero, L. R. Solvent Effects on Aromatic Nucleophilic Substitution Reactions. Part 7. Determination of the Empirical Polarity Parameter ET(30) for Dipolar Hydrogen Bond Acceptor-co-solvent (Chloroform or Dichloromethane) Mixtures. Kinetics of the Reactions of Halonitrobenzenes with Aliphatic Amines. *J. Phys. Org. Chem.* **1997**, *10*, 849–860.

(20) Mancini, P. M. E.; Terenzani, A.; Gasparri, M. G.; Vottero, L. R. Solvent Effects on Aromatic Nucleophilic Substitutions. Part 6. Kinetics of the Reaction of 1-chloro-2,4-dinitrobenzene with Piperidine in Binary Solvent Mixtures. *J. Phys. Org. Chem.* **1996**, *9*, 459–470.

(21) Martinez, R. D.; Mancini, P. M. E.; Vottero, L. R.; Nudelman, N. S. Solvent Effects on Aromatic Nucleophilic Substitutions. Part 4. Kinetics of the Reaction of 1-chloro-2,4-dinitrobenzene with Piperidine in Protic Solvents. *J. Chem. Soc., Perkin Trans. 2* **1986**, 1427–1431.

(22) Nudelman, N. S.; Mancini, P. M. E.; Martinez, R. D.; Vottero, L. R. Solvents Effects on Aromatic Nucleophilic Substitutions. Part 5. Kinetics of the Reactions of 1-fluoro-2,4-dinitrobenzene with Piperidine in Aprotic Solvents. *J. Chem. Soc., Perkin Trans. 2* **1987**, 951–954.

(23) Bunnett, J. F.; Zahler, R. E. Aromatic Nucleophilic Substitution Reactions. *Chem. Rev.* **1951**, *49*, 273–412.

(24) Crampton, M. R.; Emokpae, T. A.; Isanbo, C. Electronic and Steric Effects in the SNAr Substitution Reactions of Substituted Anilines with 2,4-dinitrophenyl 2,4,6-trinitrophenyl ether in Acetonitrile. *J. Phys. Org. Chem.* **2006**, *19*, 75–80.

(25) Crampton, M. R.; Lord, S. D. Kinetic and Equilibrium Studies of  $\sigma$ -adduct Formation and Nucleophilic Substitution in the Reactions of Trinitro-activated Benzenes with Aliphatic Amines in Acetonitrile. *J. Chem. Soc., Perkin Trans. 2* **1997**, 369–376.

(26) Castro, E. A.; Cubillos, M.; Santos, J. G.; Buján, E. I.; Remedi, M. V.; Fernández, M. A.; De Rossi, R. H. Mechanism of the Alkaline Hydrolysis of O-ethyl S-(2,4,6-trinitrophenyl)thio- and Dithiocarbonates. *J. Chem. Soc., Perkin Trans. 2* **1999**, 2603–2607.

(27) Banjoko, O.; Babatunde, I. A. Rationalization of the Conflicting Effects of Hydrogen Bond Donor Solvent on Nucleophilic Aromatic Substitution Reactions in non-polar Aprotic Solvent: Reactions of Phenyl 2,4,6-trinitrophenyl Ether with Primary and Secondary Amines in Benzene-Methanol Mixtures. *Tetrahedron* **2004**, *60*, 4645–4654.

(28) Terrier, F. *Nucleophilic Aromatic Displacement: The Influence of the Nitro Group*; Wiley: New York, 1991.

(29) Bernasconi, C. F. Kinetic Behavior of Short-lived Anionic  $\sigma$ -Complexes. *Acc. Chem. Res.* **1978**, *11*, 147–152.

(30) Bernasconi, C. F.; De Rossi, R. H.; Schmid, P. Changing Views on the Mechanism of Base Catalysis in Nucleophilic Aromatic Substitution. Kinetics of Reactions of Nitroaryl Ethers with Piperidine and with n-Butylamine in Aqueous Dioxane. *J. Am. Chem. Soc.* **1977**, *99*, 4090–4101.

(31) Miller, J. *Aromatic nucleophilic substitution*; Elsevier Publishing Co.: Amsterdam, 1968.

(32) Parr, R. G.; Szentpály, L. V.; Liu, S. Electrophilicity Index. *J. Am. Chem. Soc.* **1999**, *121*, 1922–1924.

(33) Contreras, R.; Andres, J.; Safont, V. S.; Campodonico, P.; Santos, J. G. A Theoretical Study on the Relationship Between Nucleophilicity and Ionization Potentials in Solution Phase. *J. Phys. Chem. A* **2003**, *107*, 5588–5593.

(34) Parr, R. G.; Yang, W. *Density-Functional Theory of Atoms and Molecules*; Oxford University Press, New York, 1994.

(35) Contreras, R. R.; Fuentealba, P.; Galván, M.; Pérez, P. A Direct Evaluation of Regional Fukui Functions in Molecules. *Chem. Phys. Lett.* **1999**, *304*, 405–413.

(36) Fuentealba, P.; Pérez, P.; Contreras, R. On the Condensed Fukui Function. *J. Chem. Phys.* **2000**, *113*, 2544–2551.

(37) McClelland, R. A.; Kanagasabapathy, V. M.; Banait, N. S.; Steenken, S. Reactivities of Diarylmethyl and Triarylmethyl Cations with Primary Amines in Aqueous Acetonitrile Solutions. The Importance of Amine Hydration. *J. Am. Chem. Soc.* **1992**, *114*, 1816–1823.

(38) Reed, A. E.; Curtiss, L. A.; Weinhold, F. Intermolecular Interactions from a Natural Bond Orbital, Donor-acceptor Viewpoint. *Chem. Rev.* **1988**, *88*, 899–926.

(39) Reed, A. E.; Weinhold, F. Natural Localized Molecular Orbitals. *J. Chem. Phys.* **1985**, *83*, 1736–1740.

(40) Glendening, E. D.; Reed, A. E.; Carpenter, J. E.; Weinhold, F. NBO, version 3.1.

(41) Ormazábal-Toledo, R.; Contreras, R.; Campodónico, P. R. Reactivity Indices Profile: A Companion Tool of the Potential Energy Surface for the Analysis of Reaction Mechanisms. Nucleophilic Aromatic Substitution Reactions as Test Case. *J. Org. Chem.* **2013**, *78*, 1091–1097.

(42) Ormazábal-Toledo, R.; Contreras, R.; Tapia, R. A.; Campodonico, P. R. Specific Nucleophile-Electrophile Interactions in Nucleophilic Aromatic Substitutions. *Org. Biomol. Chem.* **2013**, *11*, 2302–2309.

(43) Bunnett, J. F.; Morath, R. J. The Ortho:Para Ratio in Activation of Aromatic Nucleophilic Substitution by the Nitro Group. *J. Am. Chem. Soc.* **1955**, *77*, 5051–5055.

(44) Alabugin, I. V. Stereoelectronic Interactions in Cyclohexane, 1,3-Dioxane, 1,3-Oxathiane, and 1,3-Dithiane: W-Effect,  $\sigma_{C-X} \leftrightarrow \sigma_{C-H}^*$  Interactions, Anomeric Effect—What Is Really Important? *J. Org. Chem.* **2000**, *65*, 3910–3919.

(45) Wedel, T.; Müller, M.; Podlech, J.; Goesmann, H.; Feldmann, C. Stereoelectronic Effects in Cyclic Sulfoxides, Sulfones, and Sulfonamides: Application of the Perlin Effect to Conformational Analysis. *Chem.—Eur. J.* **2007**, *13*, 4273–4281.

(46) Garcías-Morales, C.; Martínez-Salas, S. H.; Ariza-Castolo, A. The Effect of the Nitrogen Non-Bonding Electron Pair on the NMR and X-ray in 1,3-diazaheterocycles. *Tetrahedron Lett.* **2012**, *53*, 3310–3315.

(47) Harabe, T.; Matsumoto, T.; Shioiri, T. Esters of 2,5-multisubstituted-1,3-dioxane-2-carboxylic Acid: Their Conformational Analysis and Selective Hydrolysis. *Tetrahedron* **2009**, *65*, 4044–4052.

(48) Alabugin, I. V.; Manoharan, M.; Zeidan, T. A. Homoanomeric Effects in Six-Membered Heterocycles. *J. Am. Chem. Soc.* **2003**, *125*, 14014–14031.

(49) Alabugin, I. V.; Manoharan, M. Effect of Double-Hyperconjugation on the Apparent Donor Ability of  $\sigma$ -Bonds: Insights from

the Relative Stability of  $\delta$ -Substituted Cyclohexyl Cations. *J. Org. Chem.* **2004**, *69*, 9011–9024.

(50) Frisch, M. J.; Trucks, G. W.; Schlegel, H. B.; Scuseria, G. E.; Robb, M. A.; Cheeseman, J. R.; Montgomery, J. A.; Vreven, T.; Kudin, K. N.; Burant, J. C.; et al. *Gaussian 03*, revision E.01; Gaussian Inc.; Wallingford, CT, 2004.